before it was added to the reactants. The reaction mixtures were analyzed by gas chromatography (GC) [HP-5890 GC equipped with a Supelcowax 10 fused silica column].
26. S. L. Suib, in *Recent Advances and New Horizons in Zeolite Science and Technology*, H. Chon, S. I. Woo, S. E. Park, Eds. (Studies in Surface Science and Catalysis 102, Elsevier Science, Amsterdam, 1996), pp. 47–74.
27. K. M. Parida, P. K. Satapathy, A. K. Sahoo, N. N. Das, *J. Colloid Interface Sci.* **173**, 112 (1995).
28. We acknowledge helpful discussions with M. E. Davis, A. Clearfield, C. T. Kresge, T. J. Pinnavaia, and G. D. Stucky. V. Chynwat is acknowledged for assistance with EPR experiments. We thank Y. Feng of Philips Electronic Instruments for help with HRTEM experiments. We acknowledge the U.S. Department of Energy, Office of Basic Energy Sciences, Division of Chemical Sciences, for support of this research.

2 December 1996; accepted 26 March 1997

Polarization-Enhanced NMR Spectroscopy of Biomolecules in Frozen Solution

Dennis A. Hall, Douglas C. Maus, Gary J. Gerfen, Souheil J. Inati, Lino R. Becerra,* Frederick W. Dahlquist, Robert G. Griffin†

Large dynamic nuclear polarization signal enhancements (up to a factor of 100) were obtained in the solid-state magic-angle spinning nuclear magnetic resonance (NMR) spectra of arginine and the protein T4 lysozyme in frozen glycerol-water solutions with the use of dynamic nuclear polarization. Polarization was transferred from the unpaired electrons of nitroxide free radicals to nuclear spins through microwave irradiation near the electron paramagnetic resonance frequency. This approach may be a generally applicable signal enhancement scheme for the high-resolution solid-state NMR spectroscopy of biomolecules.

Sensitivity often dictates the feasibility of solid-state NMR (*1*) studies on chemical and biological systems. The small nuclear Zeeman energy splittings result in correspondingly small nuclear spin polarizations at thermal equilibrium. For example, protons exhibit a thermal equilibrium spin polarization of <0.01% at 5 T and 300 K.

We describe here a method that can substantially improve the sensitivity of high-resolution solid-state NMR spectroscopy of biomolecular systems in frozen glycerol-water solutions. We have obtained signal enhancements of up to ~100 in the ^{13}C spectra of the amino acid arginine and ~50 in the ^{15}N spectra of the 18.7-kD protein T4-lysozyme, which correspond to a large decrease in signal averaging time or sample size requirements, or both. Alternatively, this approach may permit the routine application of the expanding repertoire of multidimensional homo- and heteronuclear recoupling techniques (*2*) for performing spectral assignments and determining structural constraints in biomolecular systems such as large soluble proteins, nucleic acids, and membrane proteins.

D. A. Hall, D. C. Maus, G. J. Gerfen, L. R. Becerra, R. G. Griffin, Francis Bitter Magnet Laboratory and Department of Chemistry, Massachusetts Institute of Technology, Cambridge, MA 02139, USA.
S. J. Inati, Department of Physics, Massachusetts Institute of Technology, Cambridge, MA 02139, USA.
F. W. Dahlquist, Department of Chemistry, University of Oregon, Eugene, OR 97403, USA.

*Present address: Massachusetts General Hospital–NMR Center, Massachusetts General Hospital, Charlestown, MA 02129, USA.
†To whom correspondence should be addressed. E-mail: griffin@ccnmr.mit.edu

Dynamic nuclear polarization (DNP) (*3*) is used to transfer the high spin polarization of unpaired electrons to coupled nuclear spins through microwave irradiation at or near the electron paramagnetic resonance (EPR) frequency. Under optimal conditions, NMR signal intensities can be increased by the ratio of the electronic and nuclear Larmor frequencies, corresponding to factors of ~660 and ~2600 for ^{1}H and ^{13}C spins, respectively.

A number of signal enhancement schemes have recently been utilized in NMR spectroscopy, including optical pumping of quantum wells (*4*), photochemically induced DNP of photosynthetic reaction centers (*5*), polarization transfer from optically polarized xenon (*4*, *6*) to surface and solution spins, and DNP of diamond, coal, and polymer systems doped with aromatic free radicals (*7*–*9*). These approaches have all proven successful for polarizing specific systems, but no method has yet been demonstrated to be generally applicable to macromolecular biological systems. Our DNP enhancement scheme uses a frozen aqueous (60:40 glycerol-water) solution doped with the nitroxide free radical 4-amino-TEMPO (2,2,6,6-tetramethyl-1-piperidinyloxy). Glycerol:water is frequently used as a cryoprotectant for protein samples in x-ray crystallography (*10*), and TEMPO and its analogs are commonly exploited for EPR spin-labeling studies on biological samples (*11*). Optimum DNP enhancement is achieved at ~40 mM radical concentration (*12*).

In the DNP–cross-polarization (CP) pulse sequence (Fig. 1), polarization is first transferred from the 4-amino-TEMPO free radical to ^{1}H spins under microwave irradiation. Irradiation on the order of the nuclear spin-lattice relaxation time (T_1) is required for maximal polarization buildup. Proton spin diffusion distributes the enhanced magnetization throughout the solvent and solute during the irradiation period. Finally, a standard CP pulse sequence (*13*) transfers the high ^{1}H polarization to rare spins (typically ^{13}C or ^{15}N) for observation. The magnetic field is chosen to maximize the experimentally determined electron-to-proton polarization transfer efficiency (*14*).

Several mechanisms of electron-proton polarization transfer exist. In these experiments using 40 mM 4-amino-TEMPO in water-glycerol, DNP primarily proceeds through a thermal mixing mechanism (*8*, *15*), in which irradiation off the center of the EPR line coupled with electron-electron cross-relaxation perturbs the electronic dipolar reservoir from thermal equilibrium. The nuclear spins become polarized through their coupling to the electronic dipolar reservoir. This coupling is induced by simultaneous spin flips of two electron spins differing in resonance frequency by the nuclear Zeeman splitting driving a nuclear spin flip (*16*). Thermal mixing involves irradiation of an allowed EPR transition, in contrast to another DNP mechanism, the solid effect, in which weak, second-order electron-nuclear spin flips are driven (*8*). Thermal mixing therefore requires less microwave power to achieve maximal enhancement, particularly in high magnetic fields where the probability of the solid effect transition is severely attenuated.

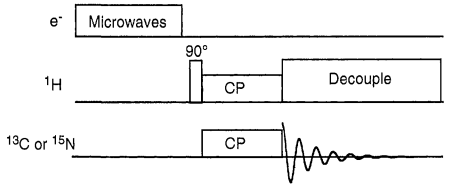

Fig. 1. Diagram of the DNP-CP pulse sequence. Initially, electronic polarization is transferred to proton spins by microwave irradiation for a period on the order of the ^{1}H T_1. The magnetic field is set to maximize the efficiency of polarization transfer. The proton polarization is then transferred to the rare nuclear spins (^{13}C or ^{15}N) by a standard cross-polarization sequence. Finally, the ^{13}C or ^{15}N spectrum is acquired while continuous-wave ^{1}H decoupling is performed.

Magic-angle spinning (MAS) (*17*) is required to obtain high-resolution solid-state NMR spectra. Although MAS techniques are conventionally performed at temperatures above 100 K, the efficiency of the DNP effect increases significantly at low temperature for two major reasons: The leakage of enhanced proton polarization to the lattice is attenuated as T_1 increases, and electron-electron cross-relaxation is more efficient as T_{1e} increases (*18*). Our experiments use a DNP-MAS probe that employs helium as the spinning and cooling gas and can achieve spinning speeds up to 5 kHz and temperatures as low as 25 K (*19*, *20*), where the proton T_1 of the 4-amino-TEMPO–water-glycerol system is greater than 30 s, as compared with 10 s or less at temperatures above 100 K.

DNP experiments have typically been limited to low magnetic fields (<1.4 T, corresponding to <40 GHz for EPR and <60 MHz for ^{1}H NMR), primarily because of the lack of high-frequency microwave sources that possess sufficient output power and have extended operating lifetimes (*21*). We have therefore constructed a custom-designed gyrotron (or cyclotron resonance maser) oscillator (*22*) capable of producing up to 100 W of 140 GHz irradiation under conditions suitable for DNP experiments at 5 T (140 GHz for EPR and 211 MHz for ^{1}H NMR) (*23*), which affords improved NMR resolution and sensitivity over lower magnetic fields.

Using DNP-CP, we have achieved signal enhancements of up to ~100 in the MAS spectra of several solutes in the 4-amino-TEMPO–water-glycerol system. As one example, the top spectrum of Fig. 2 shows an enhancement of ~20 of the ^{13}C DNP-CP MAS spectrum of uniformly ^{13}C,^{15}N-labeled arginine (30 mg/ml) in frozen solution at 55 K (*24*). The bottom spectrum was taken under identical conditions with no microwave irradiation.

T4 lysozyme is a 18.7-kD, 164-residue monomeric protein necessary for the lytic growth of bacteriophage T4. Its structure has been characterized by x-ray diffraction (*25*) and solution NMR (*26*), and expression schemes have been developed for the production of isotopically labeled samples (*26*). Enhancements of approximately 50 were observed in the CP-MAS spectrum of a 1 mM buffered solution of ^{15}N-Ala–labeled T4 lysozyme in TEMPO-water-glycerol at 40 K (Fig. 3). Enhancements of this magnitude may enable the use of newly developed solid-state NMR techniques that are designed for structural studies (*2*) but currently are difficult to apply to large biological systems.

The application of this technique to large solutes requires polarization to be delivered from radicals in solution to protons in the solute interior. The most plausible mechanism for this is proton spin diffusion (*9*). Electronic polarization from the free radical is transferred most efficiently to nearby (primarily solvent) protons, whereas direct transfer to protons within the solute should be extremely slow because of the weak dipolar interaction to the free radical. However, proton spin diffusion is fast compared to T_1, and therefore can potentially deliver enhanced polarization localized around the radical to protons throughout the solvent and solute. Typical spin diffusion constants in protonated solids range from 2×10^{-12} to 6×10^{-12} cm^2/s (*27*), which implies that proton polarization can propagate several hundred angstroms before spin-lattice relaxation causes significant polarization loss (*28*). This should be sufficiently fast to allow the application of this enhancement technique to biomolecules substantially larger than T4 lysozyme.

There are potential improvements to be made in this enhancement technique. It is possible to implement gyrotron technology to generate microwave radiation in the 200- to 600-GHz range (*21*) to take advantage of the improved NMR resolution and sensitivity at higher magnetic fields. Also, the overall utility of the DNP technique depends critically on the rate of transfer of polarization from electrons to protons. This transfer scheme requires a time on the order of the nuclear T_1 for maximal polarization transfer. Coherent DNP methods such as electron-nuclear cross-polarization (*29*) may considerably decrease this transfer time.

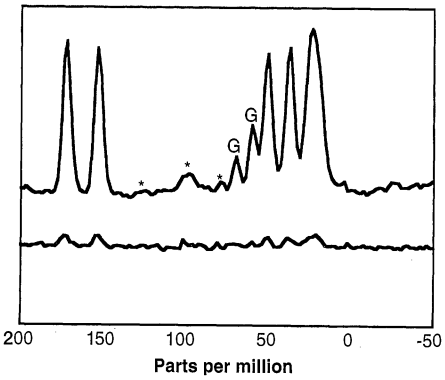

Fig. 2. DNP-CP ^{13}C solid-state MAS (3.0 kHz spin rate) spectra of fully ^{13}C-^{15}N–labeled L-Arg (30 mg/ml Arg and 40 mM 4-amino-TEMPO in 60:40 water-glycerol) at 55 K. The peaks labeled with an asterisk correspond to rotational sidebands and those labeled G correspond to the natural abundance ^{13}C glycerol peaks. Microwave irradiation (139.60 GHz) was performed for 15 s with ~1 W at the sample. Sixteen acquisitions were averaged with a 1-s recycle delay. The bottom spectrum was recorded under identical conditions with no microwave power. The magnetic field was set to maximize the positive enhancement, which is approximately 20.

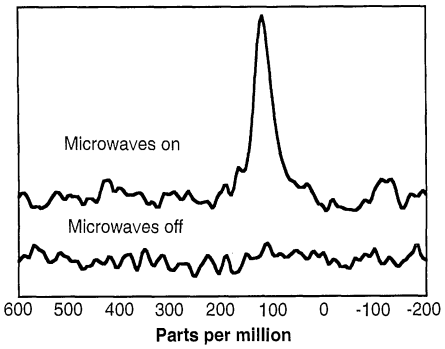

Fig. 3. DNP-CP ^{15}N solid-state MAS (3.2 kHz spin rate) spectra of ^{15}N-Ala–labeled T4 lysozyme [25 mg/ml T4 lysozyme and 40 mM 4-amino-TEMPO in 60% glycerol and 40% buffer (100 mM KCl and 30 mM potassium phosphate)] at 40 K. Microwave irradiation (139.60 GHz) was performed for 20 s with ~1 W at the sample. Sixty-four acquisitions were averaged with a 15-s recycle delay. The bottom spectrum was recorded under identical conditions with no microwave power. The magnetic field was set to maximize the positive enhancement, which is approximately 50.

REFERENCES AND NOTES

1. M. Mehring, *Principles of High-Resolution NMR in Solids* (Springer Verlag, New York, 1983); E. O. Stejskal and J. D. Memory, *High Resolution NMR in the Solid State* (Oxford Univ. Press, New York, 1994).
2. B. H. Meier, *Adv. Magn. Opt. Reson.* **18**, 1 (1994); A. Bennett, R. G. Griffin, S. Vega, *NMR Basic Princ. Prog.* **33**, 1 (1994); J. M. Griffiths and R. G. Griffin, *Anal. Chim. Acta* **283**, 1081 (1993).
3. A. Abragam, *The Principles of Nuclear Magnetism* (Clarendon, Oxford, England, 1961); C. P. Slichter, *Principles of Magnetic Resonance* (Springer-Verlag, Berlin, 1989).
4. R. Tycko and J. A. Reimer, *J. Phys. Chem.* **100**, 13240 (1996).
5. M. G. Zysmilich and A. McDermott, *J. Am. Chem. Soc.* **116**, 8362 (1994).
6. G. Navon *et al.*, *Science* **271**, 1848 (1996).
7. J. Zhou *et al.*, *Solid State Nucl. Magn. Reson.* **3**, 339 (1994); R. A. Wind, R. Lewis, H. Lock, G. E. Maciel, in *Advances in Chemistry*, R. E. Botto and Y. Sanada, Eds. (American Chemical Society, Washington, DC, 1993), pp. 1–26; L. R. Becerra, G. J. Gerfen, R. J. Temkin, D. J. Singel, R. G. Griffin, *Phys. Rev. Lett.* **71**, 3561 (1993); D. J. Singel, H. Seidel, R. D. Kendrick, C. S. Yannoni, *J. Magn. Reson.* **81**, 145 (1989).
8. R. A. Wind, M. J. Duijvestijn, C. van der Lugt, A. Manenschijn, J. Vriend, *Prog. Nucl. Magn. Reson. Spectrosc.* **17**, 33 (1985).
9. M. Afeworki, R. A. McKay, J. Schaefer, *Macromolecules* **25**, 4084 (1992).
10. P. Douzou, *Cryobiochemistry: An Introduction* (Academic Press, London, 1977).
11. L. J. Berliner, Ed., *Spin Labeling* (Academic Press, New York, 1976).
12. The DNP enhancement as a function of TEMPO concentration can be qualitatively explained as follows. At concentrations below 40 mM, both the number of unpaired electrons and the rate of electron-electron cross-relaxation are decreased, leading to less efficient polarization transfer. However, higher TEMPO concentrations lead to an increased rate of nuclear spin-lattice relaxation, which severely attenuates the DNP enhancement through polarization leakage to

the lattice.
13. A. Pines, M. G. Gibby, J. S. Waugh, *J. Chem. Phys.* **56**, 1776 (1972).
14. G. J. Gerfen, L. R. Becerra, D. A. Hall, D. J. Singel, R. G. Griffin, *ibid.* **102**, 9494 (1995).
15. W. T. Wenkebach, T. J. B. Swanenburg, N. J. Poulis, *Phys. Rep.* **14**, 181 (1974).
16. Although the TEMPO EPR line is dominated by inhomogeneous broadening, the thermal mixing effect is not necessarily precluded. Our preliminary studies indicate that electron-electron cross-relaxation across the 200 G EPR line is substantially faster than T_{1e} at low temperature, allowing the inhomogeneous EPR line to be treated as a quasi-homogeneous line. Thus, off-center irradiation of the EPR line can significantly perturb the electronic dipolar reservoir. Because the TEMPO EPR line is substantially broader than the proton resonance frequency, a flip-flop transition of two electron spins can drive a nuclear spin flip in an energy-conserving process, and thus polarize the nuclear spins. Both the microwave power and magnetic field dependences of the DNP enhancement indicate that thermal mixing is the predominant mechanism, with the solid effect making a relatively small contribution.
17. E. R. Andrew, A. Bradbury, R. G. Eades, *Nature* **182**, 1659 (1958).
18. D. A. Hall *et al.*, unpublished results.
19. This probe differs from standard MAS probes in two important respects. In order to avoid arcing due to the low breakdown voltage of helium, we used transmission line probe tuning, so that the capacitors were located outside of the probe, isolated from any helium gas. In addition, the NMR coil was coated with Teflon and all solder joints were encased in silicone sealant. The probe is capable of achieving 80-kHz proton decoupling fields for up to 40 ms at 30 K. Microwaves from the gyrotron source are delivered to the sample through a waveguide that terminates 1 cm outside the NMR coil to avoid perturbation of NMR tuning. The probe's sensitivity is comparable to standard MAS probes at this magnetic field. The MAS assembly is a standard Chemegnatics system, with 5-mm zirconia rotors. The sample volume was ~150 μl.
20. V. Macho, R. Kendrick, C. S. Yannoni, *J. Magn. Reson.* **52**, 450 (1983); A. Hackmann, H. Seidel, R. D. Kendrick, P. C. Myhre, C. S. Yannoni, *ibid.* **79**, 148 (1988).
21. P. Bhartia and I. J. Bahl, *Millimeter Wave Engineering and Applications* (Wiley, New York, 1984).
22. Unlike gyrotrons, primary millimeter-wave sources, such as the extended interaction oscillator or backward wave oscillator rely on fragile slow-wave structures to generate radiation, and thus have limited operating lifetimes under high-power operation. A gyrotron uses a electron beam in a high magnetic field to generate radiation at the electron cyclotron frequency.
23. L. R. Becerra *et al.*, *J. Magn. Reson. A* **117**, 8 (1995).
24. An important parameter affecting the signal enhancements was the sample temperature. Enhancements of ~100 were achieved at 25 K under otherwise similar experimental conditions as in Fig. 2. Enhancements at 100 K were ~5. The presence of the TEMPO free radical in the sample did not detectably increase the NMR linewidths. Experimental evidence indicates that the origin of the NMR linewidths is primarily attributable to the noncrystalline nature of the sample.
25. D. R. Rose *et al.*, *Protein Eng.* **2**, 277 (1988).
26. L. P. MacIntosh, A. J. Wand, D. F. Lowry, A. G. Redfield, F. W. Dahlquist, *Biochemistry* **29**, 6341 (1990).
27. K. Schmidt-Rohr and H.W. Spiess, *Multidimesional Solid-State NMR and Polymers* (Academic Press, London, 1994); G. C. Campbell and D. L. Vanderhart, *J. Magn. Reson.* **96**, 69 (1992).
28. The root-mean-square distance polarization propagates in a time t is approximately $(Dt)^{1/2}$, where D is the proton spin diffusion constant. This analysis assumes that the ^1H T_1 of the system is not significantly decreased by the solute.
29. H. Brunner, R. H. Fritsch, K. H. Hausser, *Z. Naturforsch.* **42a**, 1456 (1987); A. Henstra, P. Dirksen, J. Schmidt, W. T. Wenckebach, *J. Magn. Reson.* **77**, 389 (1988).
30. We thank J. Bryant for technical assistance, S. Snow for preparation of the lysozyme sample, and C. Farrar for helpful discussions. Supported by NIH (grants GM-35382, RR-00995, RR-05539, and CA-06927).

3 October 1996; accepted 10 March 1997

The Initial Domestication of *Cucurbita pepo* in the Americas 10,000 Years Ago

Bruce D. Smith

Squash seeds, peduncles, and fruit rind fragments from Archaic period stratigraphic zones of Guilá Naquitz cave in Oaxaca, Mexico, are assigned to *Cucurbita pepo* on the basis of diagnostic morphological characters and identified as representing a domesticated plant on the basis of increased seed length and peduncle diameter, as well as changes in fruit shape and color, in comparison to wild *Cucurbita* gourds. Nine accelerator mass spectrometer radiocarbon dates on these specimens document the cultivation of *C. pepo* by the inhabitants of Guilá Naquitz cave between 10,000 to 8000 calendar years ago (9000 to 7000 carbon-14 years before the present), which predates maize, beans, and other directly dated domesticates in the Americas by more than 4000 years.

The initial domestication of plants and animals and the transition from hunting and gathering to an agricultural way of life occurred independently in at least seven different primary centers of agricultural origin worldwide (*1*). In Mesoamerica, three major crop plants were first domesticated: maize (*Zea mays*), the common bean (*Phaseolus vulgaris*), and squash (*Cucurbita pepo*). Although there has been considerable recent biological research on the identity and present-day geographical range of the wild progenitors of these three major crop plants (*1*, *2*), all of the archaeological information regarding their initial domestication in Mexico comes from a series of five caves excavated in the 1950s and 1960s: Romero's and Valenzuela's caves near Ocampo, Tamaulipas (*3*); Coxcatlán and San Marcos caves in Tehuacán, Puebla (*4*); and Guilá Naquitz cave in Oaxaca (*5*). On the basis of temporally diagnostic artifacts associated with early domesticated plants in these caves, along with conventional radiocarbon age determinations on associated materials, the domestication of these three major crop plants was thought to have taken place 7000 to 10,000 calendar years before present (B.P.) (*3*–*5*). Recent reanalysis of the earliest domesticated maize, common bean, squash, and bottle gourd (*Lagenaria siceraria*) specimens from four of these five caves, however, and their direct dating by the small sample accelerator mass spectrometer (AMS) radiocarbon method, have produced much more recent ages (*3*, *6*–*8*). These much younger AMS age determinations for the earliest crop plants from Coxcatlán, Romero's, San Marcos, and Valenzuela's caves have in turn led to suggestions that the transition from hunting and gathering to incipient agricultural economies in Mesoamerica occurred much more recently than 7000 to 10,000 calendar years ago (*8*). Here I report results of the reanalysis and direct AMS dating of the earliest domesticate from Guilá Naquitz, the fifth of these Mesoamerican caves.

Guilá Naquitz cave has an uppermost late Classic period layer 20 cm thick (zone A, 620 to 740 A.D.) that is rich in storage pits and a variety of domesticated plants. Beneath zone A, four more layers (zones B through E) contain evidence of a series of short-term seasonal occupations by small family groups. These zones were dated by conventional radiocarbon age determinations to circa (ca.) 8500 to 10,500 calendar years B.P. and were thought to span the transition from hunting and gathering to incipient agriculture in the region (*5*). In the initial analysis of *Cucurbita* material from these Archaic period zones of Guilá Naquitz, the earliest apparent evidence for this agricultural transition consisted of a single seed recovered from zone D that was identified as being from domesticated *C. pepo* and believed to be 9800 years old on the basis of a conventional radiocarbon date on associated wood charcoal (*9*). Seeds and peduncles of domesticated *C. pepo* were also reported from zones B and C of the cave, along with thin rind fragments, small seeds, and small peduncles of a wild *Cucurbita* gourd.

When restudied, the *Cucurbita* assem-

Archaeobiology Program, Department of Anthropology, National Museum of Natural History, Smithsonian Institution, Washington, DC 20560, USA.